Journal of Solid State Chemistry **150,** 356–362 (2000)
doi:10.1006/jssc.1999.8604, available online at http://www.idealibrary.com on IDEAL®

Structure Analysis of Vanadyl Phosphate Intercalated with Acetone

Pavla Čapková,* Miroslava Trchová,* Vítězslav Zima,† and Henk Schenk‡

*Faculty of Mathematics and Physics, Charles University Prague, Ke Karlovu 3, CZ-12116 Prague, Czech Republic;
†Joint Laboratory of Solid State Chemistry of Academy of Sciences of the Czech Republic and University Pardubice, Pardubice, Czech Republic; and
‡Laboratory of Crystallography, University of Amsterdam, Nieuwe Achtergracht 166, NL-1018 WV Amsterdam, The Netherlands

Received May 24, 1999; in revised form November 18, 1999; accepted December 13, 1999

Structure analysis of vanadyl phosphate intercalated with acetone has been carried out using a combination of X-ray powder diffraction, infrared spectroscopy, and molecular mechanics simulations in Cerius² modeling environment. IR spectroscopy revealed the tautomerism in the interlayer space of $VOPO_4$, i.e., a partial conversion of acetone to the enrol form. Molecular simulations showed that this tautomerism leads to an increase of the orientation disorder of guest species and consequently to the increase of the disorder in layer stacking. This disorder was confirmed by X-ray powder diffraction. The basal spacing d_{001} obtained from X-ray powder diffraction is 9.04(15) Å. The average value calculated by molecular mechanics simulations $d_{001} = 9.14(25)$ Å is slightly higher due to the approximations used for the description of host–guest interaction. The positions and orientations of guest species and the mutual positions of two successive layers have been determined, including the characterization of disorder.

INTRODUCTION

Layered structures with strong intralayer and weak interlayer bonding can accommodate guest molecules in interlayer space without rearrangement or distortion of an intralayer structure. These structures represent host compounds suitable for intercalation (1–4). Intercalation affects physical and chemical properties of the structures and can thus provide us with the possibility to improve or fine tune the properties, either by a suitable combination of guest species with the host structure, or by suitable concentration of guest molecules. Anyway, the successful design of a new intercalate with desirable properties requires the full understanding of the structure–property relationship. Therefore, the structure analysis of intercalates plays a key role in this field of crystal engineering.

Intercalation can be characterized as a positioning of known molecules into a known layered crystal structure. Consequently, the structure analysis of intercalates is usually focused on the determination of positions, orientations, and arrangement of the guest molecules in the interlayer space and on the determination of the layer stacking (5). Intercalated structures usually exhibit a certain degree of disorder in their interlayer crystal packing and consequently in the layer stacking. Thus, the characterization of the disorder is an integral part of the structure analysis of the intercalates.

Structure analysis of the intercalates is usually different due to two main reasons:

- As a consequence of a structural disorder, it is not possible to prepare single crystals for the diffraction analysis, and the samples are available in powder form only.
- The powder diffraction pattern, which is affected by the disorder, is in addition affected by preferred orientation of disk-shaped particles of the intercalate.

As a result of these effects, one can observe only *00l* reflections and very weak and broad *hkl* reflections. It is evident that X-ray diffraction alone cannot solve all the specific problems of the intercalated structures. In such a case, molecular simulations combined with experimental methods (XRD, NMR, IR, and Raman spectroscopy) represent very useful complementary tools in the structural studies of intercalates.

Molecular simulations predict crystal structure and properties using energy minimization. The crystal energy in the molecular mechanics simulation is described by an empirical force field. The potential energy for the arbitrary geometry of a molecule or crystal structure is expressed as a superposition of valence (bonded) interactions and nonbonded interactions (i.e., Van der Waals, Coulomb, and hydrogen bond). The valence interactions consist of bond stretch, bond-angle bend, torsion, and inversion terms (for more details see for example Mayo *et al.* (6)). The strategy of modeling, which means the building of the initial model, the choice of the force field, and minimization conditions, is based on the preliminary results of X-ray diffraction and IR spectroscopy.

In the present work, we used molecular mechanics simulations in Cerius² modeling environment (Molecular Simulations, Inc.) in conjunction with X-ray powder diffraction and IR spectroscopy to investigate the structure of vanadyl

0022-4596/00 $35.00

phosphate intercalated with acetone. For the description of Cerius[2] software, see for example Comba and Hambley (7). This complex structure analysis provides us with the description of structure including the characterization of disorder, the character of the host–guest interactions, and the total sublimation energy.

EXPERIMENTAL

Sample Preparation and XRD Measurements

Vanadyl phosphate dihydrate was prepared by boiling a mixture of V_2O_5 in diluted H_3PO_4 under a reflux for 14 h (8). The product was filtered and washed with distilled water several times. The yellow solid was dried in air at ambient temperature. The intercalation compound of acetone with $VOPO_4$ was obtained by a reintercalation reaction of a propanol intercalate with acetone. The propanol intercalate was prepared by suspending microcrystalline $VOPO_4 \cdot 2H_2O$ (ca. 1 g) in about 10 ml of dry propanol. The reaction mixture was placed in a 15-ml glass flask equipped with a reflux condenser and put into the wave guide of a microwave generator with stirring and heating and exposed to a microwave field or 10 min (9, 10). The construction of the microwave generator was described earlier (9). After cooling, the solid product that formed was filtered off. The product (1 g) was suspended in 50 ml of dry acetone and stirred for 1 h at room temperature. The intercalate was filtered and stored over P_2O_5.

The powder data of the intercalate with an excess of acetone were measured under protection foil by means of an X-ray diffractometer (HZG-4, Germany) using Cu$K\alpha_1$ radiation ($\lambda = 1.54051$ Å) with discrimination of the Cu$K\beta$ by an Ni-filter. The Cu$K\alpha_2$ intensities were removed from the original data using Rachinger procedure in the program DIFPATAN (11). Silicon ($a = 5.43055$ Å) was used as external standard. Diffraction angles were measured in the 3–50° range in 2θ. In order to minimize preferential orientation, the following process was applied: A piece of flat glass serving as a sample holder was coated with silicone grease and then sprinkled with finely ground $VOPO_4 \cdot 2H_2O$. Vapors prepared by bubbling dry nitrogen through liquid propanol were blown on the sample. The propanol intercalate formed by this way was then blown with acetone vapors. The whole process of intercalation was continually checked by X-ray diffraction. This method of sample preparation eliminates the preferred orientation of flat powder particles. The measured diffraction pattern is shown in Fig. 1.

The character of the X-ray powder pattern exhibits the features, characteristic for disordered layered structures, which make the structure analysis extremely difficult:

- The strong preferred orientation of disk-shaped particles with predominant *00l* reflections.

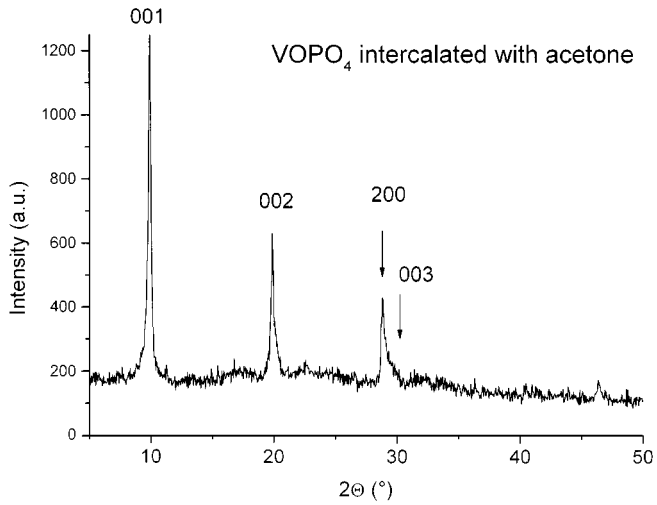

FIG. 1. X-ray powder diffraction pattern of vanadyl phosphate intercalated with acetone, where only three basal reflections are observable.

- The width of basal reflections *00l* exceeds the instrumental broadening and indicates certain fluctuations in basal spacing due to the irregularity in the interlayer crystal packing.
- The broadening of *hk0* and *hkl* reflections indicating the disorder in layer stacking.

The X-ray diffraction pattern was analyzed using the program DIFPATAN (11). Asymmetric Pearson function has been used to fit the line profiles and to decompose the overlapping lines 200/003. The basal spacing obtained by extrapolation method (12) was 9.04(15) Å. The *00l* line widths FWHM (full with at half maximum) were used to analyze the interlayer microstrain, due to the inhomogeneity of basal spacing. The fluctuation range of basal spacing found by Williams–Hall method (13) was 8.89–9.19 Å.

IR Spectroscopy

Infrared spectroscopic measurements were carried out using a NICOLET IMPACT 400 Fourier transforms infrared (FTIR) spectrophotometer in a H_2O-purged environment. An ambient-temperature deuterated triglycine sulfate (DTGS) detector was used for the wavelength range from 400 to 4000 cm^{-1}. The baseline horizontal attenuated total reflection (ATR) accessory with ZnSe crystal ($n = 2.4$ at 1000 cm^{-1}) was used for the measurements of the infrared spectra of the samples. In our experiments, the effective path length was approximately a few μm (angle of incidence, 60°; number of reflections, 7). The ATR correction was made to eliminate the dependence of the effective path length on the wavelength. The measurements of the vibration spectra of each compound were repeated three times using three different samples of the same material. No changes of the studied spectral features have been observed.

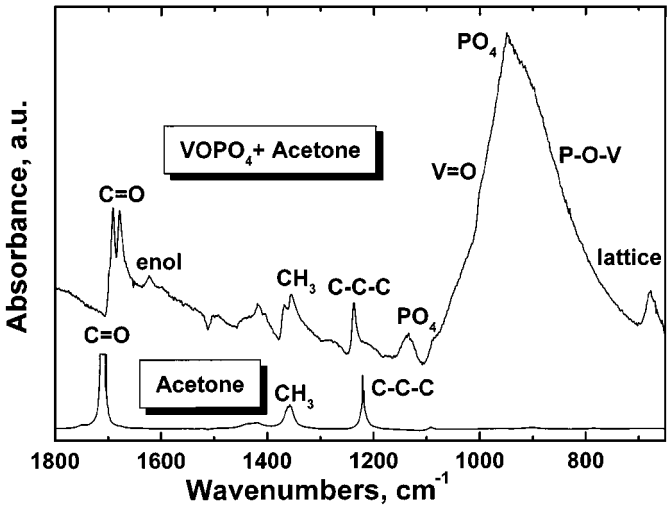

FIG. 2. Infrared spectra of the pristine acetone and the vanadyl phosphate, intercalated with acetone.

Figure 2 shows the infrared spectrum of the pristine acetone and vanadyl phosphate intercalated with acetone. Comparing these two spectra we can observe a slight shift of the C–C–C asymmetric stretching band from 1223 cm^{-1} in pristine acetone to 1239 cm^{-1} in the intercalate due to the crystal field in the interlayer space. According to Silverstein (14) the configuration in which two methyl groups are attached to the same carbon atom exhibits a distinctive absorption band in C–H bending region. This band is split due to the interactions between the in-phase and out-of-phase symmetrical CH_3 bending of the methyl groups attached to the same carbon atom. Two peaks of almost equal intensity at 1362 and 1357 cm^{-1} are observed in the pristine acetone. This splitting is more pronounced in the intercalate (1368/1356 cm^{-1}), where the two different methyl groups reside in different environments in the interlayer space. Two distinct bands corresponding to asymmetrical bending vibration of CH_3 are observed at 1438 and 1421 cm^{-1} in the pristine acetone. This splitting is more pronounced in the intercalate, due to the reason mentioned above (Fig. 2). In addition, this profile of the band between 1400 and 1450 cm^{-1} is affected with the presence of enol-form. According to (14, 15) the scissoring band of CH_2 occurs between 1400 and 1450 cm^{-1}.

The IR spectra should be divided into two parts for the present analysis. The first part at low wavenumbers 650–1500 cm^{-1} shows the same character of guest molecules in the pristine acetone and in the intercalate, with only a slight shift or more pronounced doublet splitting. The second part at high wave numbers shows the changes going from the pristine acetone to the acetone in intercalate. First of all, the C=O stretching vibration band observed at 1712 cm^{-1} in the pristine acetone is split (1690/1680 cm^{-1}) in the intercalate, probably due to the anchoring of C=O oxygen to the vanadium in $VOPO_4$ host layer. The most important difference between the two spectra in Fig. 2 is the presence of the new band at 1622 cm^{-1} in the IR spectrum of intercalate. According to (14, 15) this band corresponds to the C=C bond of enol form, which can occur in the interlayer space of $VOPO_4$.

In order to estimate the possible changes in host layers during the intercalation, four characteristic absorption bands corresponding to the $VOPO_4$ layers were used for the estimation of the intercalation effect on the host structure:

1. PO_4 asymmetric stretching, observable at 1143 cm^{-1} in the host structure and at 1133 cm^{-1} in the intercalate. The band positions for the host structure were taken from our previous work (16).
2. V=O stretching mode, observable at 995 cm^{-1} in the host structure and at 1002 cm^{-1} in the intercalate (only a shoulder).
3. PO_4 symmetric stretching overlapped with a P–O–V deformation band. This broadened band has the center of gravity in the same position at about 920 cm^{-1} in the host and intercalated structure.
4. Lattice vibrations at 681 cm^{-1} in the host structure and at 678 cm^{-1} in intercalate.

The comparison of IR spectra for acetone, host structure, and intercalate showed only slight changes in positions of bands corresponding to acetone molecules and $VOPO_4$ layers; that means that besides the occurrence of the enol-form, no significant changes of the host structure and guest molecules can be observed after intercalation. This conclusion is extremely important for the strategy of modeling.

STRATEGY OF MODELING

Strategy of modeling, i.e., the building of the initial models, the set up of energy expression, choice of the force field, and conditions of energy minimization, was based on the experiment. The initial model of intercalate $VOPO_4 \cdot CH_3COCH_3$ was built using the known structure data for the host compound $VOPO_4 \cdot 2H_2O$. The host structure was determined by Tietze (17) from single-crystal X-ray diffraction as a tetragonal, space group $P4/nmm$ with $a = 6.202$, $c = 7.41$ Å and $z = 2$. Tachez *et al.* (18) presented the structure refinement of the deuterated compound $VOPO_4 \cdot 2D_2O$ based on neutron powder diffraction data: space group $P4/n$, $a = 6.2154(2)$, and $c = 7.4029(7)$ Å. The host structure of vanadyl phosphate dihydrate consists of sheets of distorted VO_6 octahedra and PO_4 tetahedra linked by shared oxygen atoms (see Fig. 3). Two differently bonded water molecules in the interlayer space give rise to the network of hydrogen bonds, linking the $VOPO_4$ sheets together. The first water molecule attached to vanadium is hydrogen bonded to the second water molecule, which is hydrogen bonded to PO_4 oxygens. In the present initial model we used the structure data of Tachez *et al.* (18). The

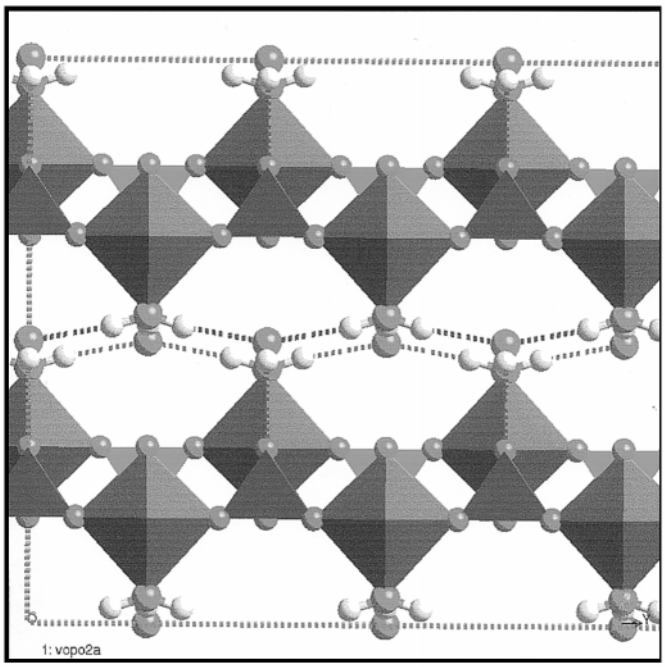

FIG. 3. The host structure of vanadyl phosphate, with the interlayer water molecules. Hydrogen bonds between water molecules are marked with dotted lines.

$VOPO_4$ layers in the initial model were removed to the interlayer distance 9 Å and the water molecules were replaced by the intercalating species. Creating the modeling strategy we took into account the following experimental results:

• From X-ray powder diffraction of the intercalate, we obtained the basal spacing $d = 9.04$ Å. The broadening of *00l* line profiles shows the microstrain in the interlayer accompanied with the inhomogeneity of basal spacing and indicating an interlayer disorder. The *200* reflection observable in the diffraction pattern shows the *a* parameter of 6.21 Å unchanged in comparison with the host structure. Weak and broadened *hkl* reflections in the diffraction pattern of intercalate indicate a disorder in the layer stacking.

• IR spectra of the intercalate and the host structure exhibit nearly the same positions of bands corresponding to the symmetric and asymmetric PO_4 stretching modes to the V=O stretching and lattice vibration mode. That means no significant distortions of the $VOPO_4$ layers are caused by intercalation. The absorption bands corresponding to acetone have nearly the same or slightly shifted positions in the IR spectrum of the intercalate in comparison with the spectrum of the pristine acetone. The presence of the absorption band of enol-form was taken into account in the strategy of modeling.

These experimental results led us to the conclusion that in our calculations the host layers and guest molecules can be treated as rigid bodies (with sufficiently good approximation) and that the host–guest interactions have a nonbond character. That means the Crystal Packer module in the Cerius[2] modeling environment can be used, which leads to the significant reduction of CPU time necessary for the calculations. Taking into account the nonbond host–guest interactions only, we are neglecting the $V–O_{acetone}$ bonding forces between the vanadium and acetone oxygen $O_{acetone}$. The possible error caused by this approximation should be noticeable in the $V–O_{acetone}$ distance and consequently in the basal spacing. This effect will be discussed later in Results.

Crystal Packer is a computational module that estimates the total sublimation energy and packing of molecular crystals. Energy calculations in Crystal Packer take into account the nonbond terms only, i.e., van der Waals interactions (VDW), Coulombic interactions (COUL), hydrogen bonding (H-B), internal rotations, and hydrostatic pressure. The asymmetric unit of the crystal structure is divided into fragment-based rigid units. Nonbond (VDW, COUL, and H-B) energies are calculated between the rigid units. During the energy minimization, the rigid units can be translated and rotated and the unit cell parameters varied. The Ewald summation method is used to calculate the Coulomb energy in a crystal structure (Karasawa and Goddard III (19)). The Ewald sum constant was 0.5 $Å^{-1}$. The minimum charge taken into the Ewald sum was 0.00001e. All atom pairs with separations less than 10 Å were included in the real-space part of the Ewald sum, and all reciprocal-lattice vectors with lengths less than 0.5 $Å^{-1}$ were included in the reciprocal part of the Ewald summation. Charges in the crystal are calculated in Cerius[2] using the *QEq*-method (Charge equilibrium approach). This method is described in detail in the original work of Rappé and Goddard III (20). For VDW we used the well-known Lennard–Jones functional form, with the arithmetical radius combination rule. A nonbond cut-off distance for the VDW interactions was 7.0 Å. There are three force fields available in Crystal Packer for VDW parameters: Tripos (21), Universal (22), and Dreiding (23). In minimizing a very low density cell, the intermolecular distances may be greater than the nonbond cut-off distance and no attractive interunit forces are calculated. However, by applying an external pressure at the start of the minimization, one can bring the rigid units into closer contact. The external pressure 50 kbar was applied for the first minimization and then the external pressure was removed and new minimization started. Three sets of initial models have been built for the molecular mechanics simulations, as follows.

I. Model-A. Pure acetone in the interlayer space. Cell parameters: $a = b = 6.21$ Å, $\alpha = \beta = \gamma = 90°$, and $c = 9$ Å and with two formula units $VOPO_4 \cdot CH_3COCH_3$ per one unit cell. Space group *P*1 allows the variation of parameters α, β, and *c* during energy minimization. The parameters *a*, *b*,

and γ were fixed in agreement with the assumption of rigid layers. Three rigid units were assigned to one unit cell for the energy minimization: two acetone molecules and one host layer.

II. Model-AE1. Acetone with 25% of enol-form in the interlayer space. Space group $P1$, supercell $2ax2bx1c$, i.e., supercell parameters $A = B = 12.42$ Å, $B = 2b$, $C = 9$ Å (*parameters a, b, c, α, β, γ*, were the same as in Model-A) and the supercell content: $8(VOPO_4)\cdot 6(CH_3COCH_3)\cdot 2\,C_2{=}C(OH)CH_3$ with two enol-molecules per supercell. Rigid units were 6 acetone molecules, 2 enol molecules, and host layer.

III. Model-AE2. Acetone with 12.5% of enol-form in the interlayer space. Space group $P1$, the same supercell as in Model-AE1, with the supercell content: $8(VOPO_4)\cdot 7(CH_3COCH_3)\cdot CH_2{=}C(OH)CH_3$. Rigid units were 7 acetone molecules, 1 enol molecule, and host layer.

RESULTS AND DISCUSSION

Model-A

A series of initial models with different initial positions and orientations of acetone molecules in the interlayer space have been prepared for modeling. The results of energy minimization for all these models led to the structure model illustrated in Fig. 4. Two sets of the VDW parameters were used in the present calculations from the Universal and Tripos force fields. Both sets of the parameters give the same arrangement of the guest molecules; however, the Tripos VDW parameters led to better agreement of the calculated and measured basal spacing: d(calc) = 8.98 Å and d(exp) = 9.04 Å. The basal spacing in all calculated models varied within the 8.88–9.07 Å range, and the mutual position of the two successive layers exhibits shift in *100* direction with respect to the tetragonal host lattice (see Fig. 5). The shift vector σ characterizing the position of the two successive layers has the main component in a direction $\sigma_a =$ 0.25–0.58 Å; that means $\Delta\sigma_a = 0.33$ Å while the component σ_b is in the 0.001–0.01 Å range.

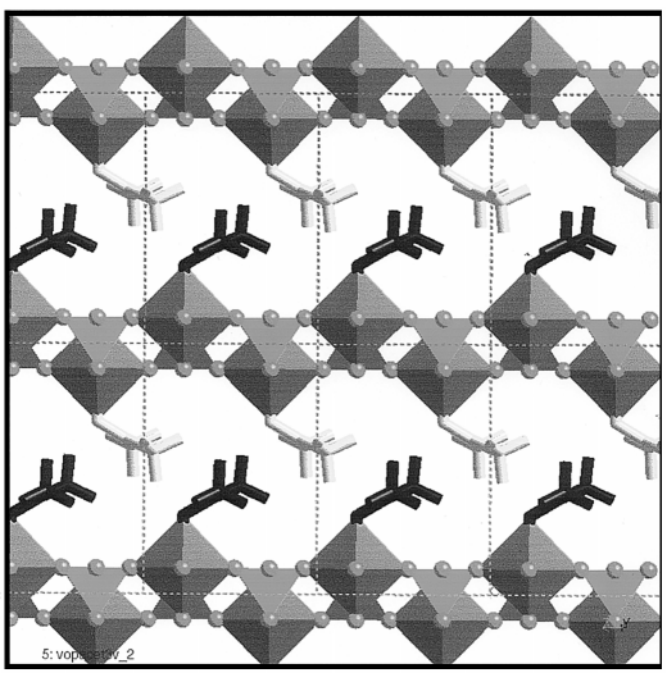

FIG. 4. The arrangement of pure acetone in the interlayer space of $VOPO_4$. The oxygen atoms of acetone complete the vanadium octahedra.

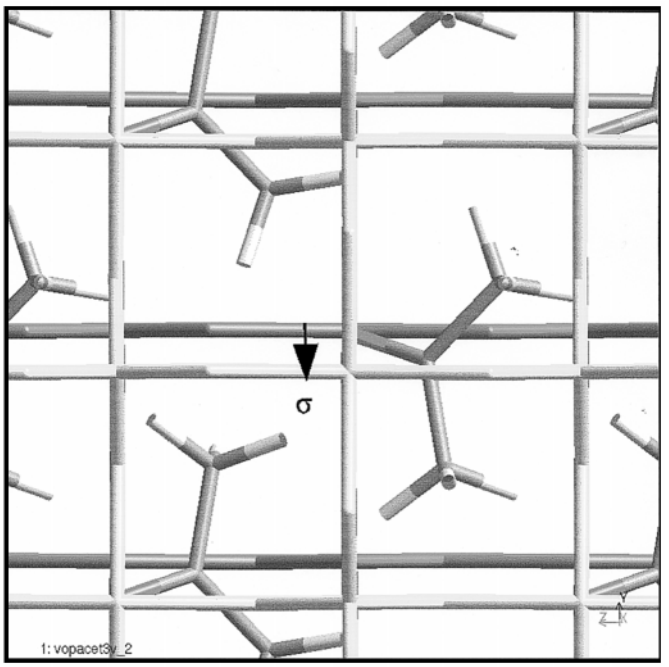

FIG. 5. Mutual positions of the two successive $VOPO_4$ layers, schematically drawn as cylinders, with the positions of interlayer acetone molecules. The shift vector σ is denoted by arrow (Model-A with acetone molecules only).

The acetone molecules in the minimized models are anchored to vanadium with their oxygen O_{ac} to complete the VO_6 octahedra and to replace water oxygen in the host structure. This is in agreement with the IR spectroscopy results, which show the V=O stretching band at nearly the same position in the intercalated and host structures, indicating the same coordination of vanadium in host structure and intercalate. The average calculated V–O_{acet} distance is 2.33 Å, while the V–O_{water} distance in hydrate is 2.23 Å. The calculated V–O_{acet} distance may be influenced by the neglect of V–O bond interaction. However, the comparison of calculated and experimental basal spacing shows that the effect caused by the neglect of V–O bond interaction is negligible (within the limits of experimental error).

Acetone molecules attached to the lower and upper sheets of $VOPO_4$ are arranged in two partially overlapping layers

and the C–C–C plane of acetone is inclined to the $VOPO_4$ sheet. The average C–C–C inclination angle varies within the 29.4–29.8° range, giving the average value is 29.6°. The inclined C–C–C planes of acetone molecules are slightly rotated around C=O bonds. As a result of this rotation the methyl groups in one acetone molecule have slightly different positions and orientations with respect to the $VOPO_4$ sheet. This effect can explain the enlarged splitting of CH_3 bending modes in the intercalate in comparison with the pristine acetone. The total sublimation energy per one unit cell 135.14 kcal/mol consists of two parts: van der Waals (20.42 kcal/mol) and electrostatic (134.72 kcal/mol) contribution.

Model-AE1 and Model-AE2

The result of modeling for the models with 25 and 12.5% of enol-form in the unit cell shows a higher degree of disorder in the interlayer space, as one can see from Fig. 6. Comparing with Fig. 4, one can see the slightly different orientation of individual guest species acetone and enol-molecules with respect to layers. The C–C–C inclination angle of acetone molecules varies within 28.8–31.1°, and in case of the enol-form within 24.3–28.0°. (The C–C–C inclination angle was obtained by averaging over the aceton and enol molecules in one supercell and over the series of minimized models for: Model-AE1 and -AE2.) Comparing these values with those from the Model-A and comparing the ranges, it is evident that enol-form causes a higher disorder in the structure of intercalate. This orientation disorder leads to the higher degree of disorder in layer stacking. The magnitude of the shift vector σ in *001* direction varied within 0.37–0.78 Å and the basal spacing varied within 9.29–9.39 Å for models with 12.5 and 25% enol-form. The enol molecules are anchored to vanadium with their oxygen O_{enol} to complete the VO_6 octahedra and to replace water oxygen in the host structure. The average value of the calculated $V–O_{enol}$ distance is 2.40 Å, which is higher than the calculated $V–O_{acet}$ distance.

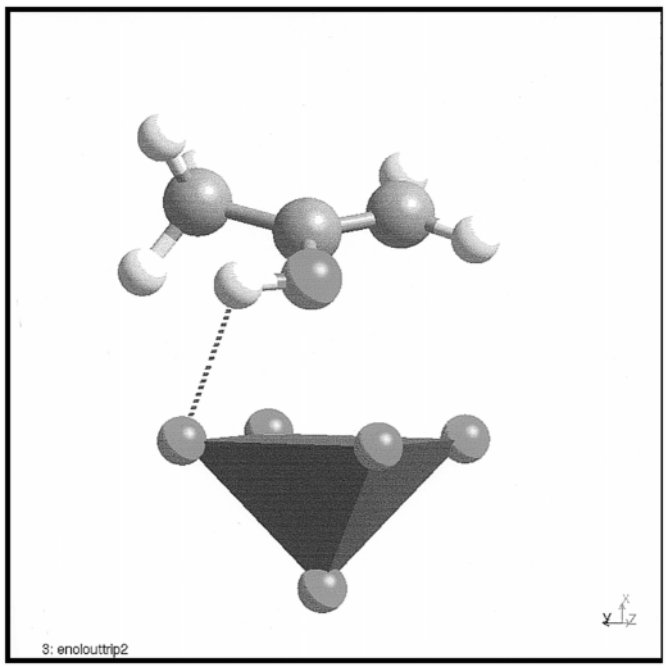

FIG. 7. The anchoring of enol-molecule to the vanadium octahedron.

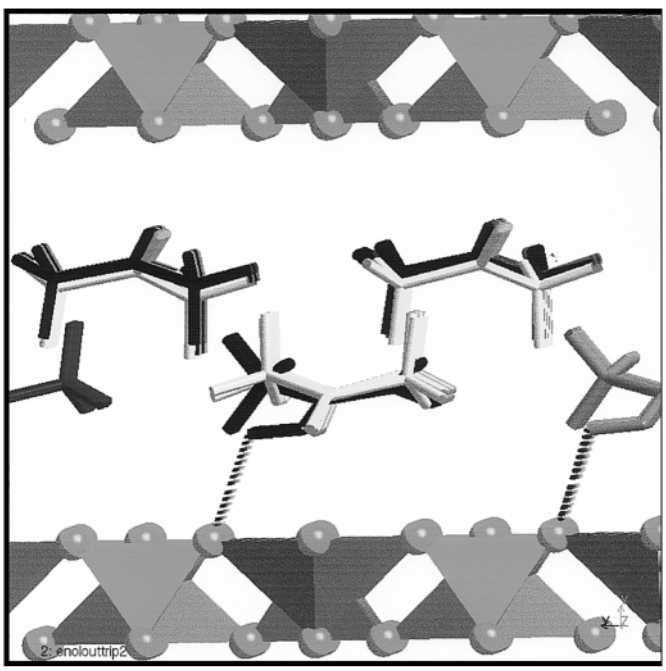

FIG. 6. The arrangement of the acetone and enol-molecules in the interlayer space of $VOPO_4$. The hydrogen bonds of the enol–OH groups to PO_4 oxygen are marked with dotted lines (Model-AE1).

The character of the diffraction pattern, that means the *00l* line broadening indicating the range of basal spacing 8.89–9.19 Å and the *hkl* broadening, shows that the disorder in real samples is caused by the presence of domains with various concentration of enol-form and with a certain degree of orientation disorder of guest molecules and consequently with internal strain in the interlayer accompanied with the corresponding range of basal spacing. Taking into account all the calculated models in the three sets of type Models A, AE1, and AE2, we obtained the average basal spacing 9.14 Å, which is in good agreement with the experimental value, 9.04(15) Å, within the limits of experimental error.

CONCLUSIONS

Present results showed that the combination of X-ray diffraction and IR spectroscopy with molecular mechanics

simulations can provide us with the structure characterization of the intercalated layered structure, which is usually partially disordered, and consequently the conventional structure analysis based on diffraction method is impossible in such a case. As a result of this complex structure analysis we can get the detailed model of structure including the characterization of the disorder and the information about the character of the host–guest interactions. Present results also showed the importance of the experiment for the strategy of modeling and for the confirmation of the results of modeling.

ACKNOWLEDGMENTS

The authors are grateful to Professor J. Votinský from the University of Pardubice for fruitful discussions. This work was supported by the grant agency of the Czech Republic GAČR, Grant 203/97/1010, and the grant agency of Charles University Prague, Grant 37/97/B.

REFERENCES

1. G. Alberti, U. Costantino, F. Marmottini, R. Vivani, and P. Zappelli, *in* "Pillared Layered Structures" (I. V. Mitchell, Ed.). Elsevier Applied Science, London, New York, 1996.
2. A. Clearfield, *in* "Inorganic Ion Exchange Materials," Chap. 1–3. CRC Press, Boca Raton, FL, 1982.
3. A. Clearfield, G. H. Nancollas, and R. H. Blessing, *in* "Ion Exchange and Solvent Extraction" (J. A. Marinsky and Y. Marcus, Eds.), Vol. 5, Chap. 1. Dekker, New York, 1973.
4. U. Costantino, *J. Inorg. Nucl. Chem.* **43,** 1895 (1981).
5. P. Čapková, D. Janeba, L. Beneš, K. Melánová, and H. Schenk, *J. Mol. Model.* **4,** 150 (1998).
6. J. S. Mayo, B. D. Olafson, and W. A. J. Goddard III, *J. Phys. Chem.* **94,** 8897 (1990).
7. P. Comba and T. W. Hambley, *in* "Molecular Modelling," Chap. 1 and Appendices. VCH Verlagsgesellschaft mbH. NY, 1995.
8. G. Ladwig, *Z. Anorg. Allg. Chem.* **338,** 266 (1965).
9. L. Beneš, K. Melánová, V. Zima, J. Kalousová, and J. Votinský, *Inorg. Chem.* **36,** 2850 (1997).
10. L. Beneš, K. Melánová, V. Zima, and J. Votinský, *J. Solid State Chem.* **141,** 64 (1998).
11. R. Kužel j.r., "DIFPATAN computer program," Faculty of Mathematics and Physics, Charles University Prague, Czech Republic.
12. H. P. Klug and L. E. Alexander, "X-ray Diffraction Procedures for Polycrystalline and Amorphous Materials," (Chap. 9, Wiley, New York, 1971.
13. V. Valvoda, M. Polcarová, and P. Lukáč, "Základy strukturní analýzy" Charles University, Prague, 1992.
14. R. M. Silverstein, C. G. Bassler, and T. C. Morrill, "Spectrometric Identification of Organic Compounds" (D. Savicky and J. Stiefel, Eds.), pp. 103–115. Wiley, New York, 1998.
15. S. Holly and P. Sohar, "Absorption Spectra in the Infrared Region (Theoretical and Technical Introduction)" (L. Lang and W. H. Prichord, Eds.), pp. 56–61. Academiai Kiado, Budapest, 1975.
16. P. Čapková, M. Trchová, P. Matějka, J. Votinský, and H. Schnek, *J. Mol. Model* **4,** 284 (1998).
17. H. R. Tietze, *Aust. J. Chem.* **34,** 2035 (1981).
18. M. Tachez, F. Theobald, J. Bernard, and A. W. Hewat, *Rev. Chem. Mineral.* **19,** 291 (1982).
19. N. Karasawa and W. A. Goddard III, *J. Phys. Chem.* **93,** 7320 (1989).
20. A. K. Rappé and W. A. Goddard III, *J. Phys. Chem.* **95,** 3358 (1991).
21. M. Clark, R. D. Cramer III, and N. Van Opdenbosh, *J. Comp. Chem.* **10,** 982 (1989).
22. A. K. Rappé and W. A. Goddard III, *J. Phys. Chem.* **95,** 3358 (1991).
23. L. S. Mayo, B. D. Olafson, and W. A. Goddard III, *J. Phys. Chem.* **94,** 8897 (1990).